Plasticized Starch/Tunicin Whiskers Nanocomposites. 1. Structural Analysis

ARTICLE *in* MACROMOLECULES · OCTOBER 2000

Impact Factor: 5.8 · DOI: 10.1021/ma0008701

2 AUTHORS:

Neus Anglès
John Wiley And Sons
29 PUBLICATIONS **1,120** CITATIONS
SEE PROFILE

Alain Dufresne
Grenoble Institute of Technology
313 PUBLICATIONS **15,348** CITATIONS
SEE PROFILE

Plasticized Starch/Tunicin Whiskers Nanocomposites. 1. Structural Analysis

M. Neus Anglès and Alain Dufresne*

Centre de Recherches sur les Macromolécules Végétales (CERMAV-CNRS), Université Joseph Fourier, BP 53, F-38041 Grenoble Cedex 9, France

Received May 19, 2000

ABSTRACT: Nanocomposite materials were obtained using glycerol plasticized starch as the matrix and a colloidal suspension of cellulose whiskers as the reinforcing phase. The cellulose whiskers, prepared from tunicin, consisted of slender parallelepiped rods with a high aspect ratio. After mixing the raw materials and gelatinization of starch, the resulting suspension was cast and evaporated under vacuum. The composites were conditioned at various moisture contents in order to evaluate the effect of this parameter on the composite structure. The resulting films were characterized using scanning electron microscopy, differential scanning calorimetry, water absorption experiments, and wide-angle X-ray scattering. An accumulation of plasticizer in the cellulose/amylopectin interfacial zones was evidenced. The specific behavior of amylopectin chains located near the interface in the presence of cellulose probably led to a transcrystallization phenomenon of amylopectin on cellulose whiskers surface.

Introduction

There is a growing interest in the nonfood usage of starch-based products for applications in which synthetic polymers have traditionally been the materials of choice. Especially, the incorporation of granular starch as filler[1−3] or disrupted starch granules[4−8] into commodity plastics has generated worldwide a considerable attention in using starch to enhance biodegradability of plastic materials. Starch is the cheapest biopolymer, and it is totally biodegradable. It is also available in large quantities from several renewable plant sources produced in abundance beyond available markets. But, in starch-filled plastics, bacteria and fungi digest the starch fraction, and the remainder one is not degraded by any biological activity, representing up to 95% of the whole material.

A second generation of starch-based materials have been studied in which granular starch must be mixed with enough nonaqueous plasticizer (generally polyols, such as glycerol) to enable melting below the decomposition temperature of starch. This procedure yields a product in which starch forms a continuous polymeric entangled phase or a completely disordered molecular structure of the granular starch. This type of starch is known as thermoplastic starch (TPS)[9] or destructured starch (DS),[10] which can be manufactured using technology already developed for the production of synthetic plastics, thus representing a minor investment. The potential advantages of such materials, apart from their environmental gains, are the abundant availability of the raw materials from renewable resources, not depending on fossil sources, and also their low cost, which represents both economic and social benefits.

By itself, starch is a poor choice as a replacement for any plastic. It is mostly water-soluble, difficult to process, and brittle when used without plasticizer addition. Furthermore, its mechanical properties are very sensitive to the moisture content, which is difficult to control.

* To whom correspondence should be addressed. E-mail: Alain.Dufresne@cermav.cnrs.fr.

In previous works[11,12] composite materials were obtained from a potato pulp cellulose microfibrils suspension and an aqueous suspension of gelatinized potato starch as the matrix. Improved thermomechanical properties and a decrease of the water sensitivity of these systems were reported. However, the understanding of the phenomena involved in these improvements requires the processing and the characterization of model systems. Such model systems can be obtained using cellulose whiskers as a model cellulosic filler.

Physical incorporation of cellulose whiskers, and especially tunicin whiskers, as cellulosic model filler into polymeric matrix for the processing of model composites has been largely used, since the first announcement of using cellulose whiskers as a reinforcing phase.[13] This extensive use[14−18] can be explained by the regular shape, high aspect ratio, and monocrystalline nature of cellulose whiskers. The main problem associated with the modeling of the starch-based materials is the presence of four components (starch, cellulose, main plasticizer, and water). These components can be found in different phases (amorphous, crystalline, liquid). In addition, competitive interactions should occur between these components. All these factors make the system largely more complex than in the case of unplasticized amorphous or semicrystalline matrix filled with cellulose whiskers.

In the present study, the structure of the complex system obtained from plasticized starch reinforced with tunicin whiskers is analyzed as a function of cellulose and relative humidity content. From this knowledge, the mechanical behavior of these materials will be analyzed in the second part of the paper.[19]

Experimental Section

Starch Matrix. The starch gels were prepared by gelatinization of waxy maize starch (almost pure amylopectin, amylose content is lower than 1%) kindly supplied by Roquette S.A. (Lestrem, France), dispersed in a mixture of water and glycerol (Prolabo, 98% purity). Gels contained 10 wt % waxy maize starch, 5 wt % glycerol, and 85 wt % water. These ratios were the average values found in the literature for the processing of TPS.[20−28] The gelatinization was performed in a

10.1021/ma0008701 CCC: $19.00
Published on Web 10/07/2000

stirred autoclave reactor operating at 160 °C for 5 min. These conditions were optimized by varying systematically the processing temperature and duration in the ranges 150−190 °C and 5−60 min, respectively. The criteria for the optimization of the process were the complete disappearance of ghosts within the starch gel and the avoiding of starch degradation. The determination of the disappearance of ghosts was carried out by optical microscopy, and the observation of starch degradation was checked by visual inspection of films appearance, degradation leading to a tanning of resulting films. After mixing, the suspension was degassed under vacuum in order to remove the remaining air and cast in a Teflon mold stored at 70 °C under vacuum to allow water evaporation.

Cellulose Whiskers. Cellulose microcrystals, or whiskers, were extracted from tunicate (a sea animal). The mantle of tunicate is formed of cellulosic microfibrils (tunicin) particularly well organized and therefore highly crystalline. Colloidal suspensions of whiskers in water were prepared as described elsewhere.[13,14,29,30] Mantels were first cut into small fragments that were deproteinized by three successive bleaching treatments, following the method of Wise et al.[29] The bleached mantle (the tunicin) was then disintegrated in water with a Waring blender (at a concentration of 5 wt %). The resulting aqueous tunicin suspension was mixed with H_2SO_4 to reach a final acid/water concentration of 55 wt %. Hydrolysis conditions were 60 °C for 20 min under strong stirring. The suspension was neutralized and washed with water. After sonication a dispersion of well individualized cellulose whiskers resulted, which did not sediment or flocculate as a consequence of surface sulfate groups created during the sulfuric acid treatment.[30]

Film Processing. The starting products (starch + glycerol + water + cellulose whiskers suspension) were mixed in order to obtain composite films with a homogeneous dispersion and with different compositions. The glycerol content was fixed at 33% (dry basis of starch matrix). The cellulose whiskers content was varied from 0 to 25 wt % (cellulose/starch + glycerol). Similar processing conditions as those described for the unfilled starch matrix were used to gelatinize starch and to process nanocomposite films. Native waxy maize was gelatinized directly in the presence of water, plasticizer, and cellulose.

Film Conditioning. Starch and cellulose are highly hygroscopic materials. The structure and therefore the properties of these materials are strongly related to the water content.[31−36] The moisture content of the nanocomposite films was achieved by conditioning the samples at room temperature in desiccators at controlled humidities containing saturated salt solutions. Six relative humidity (RH) conditions at 20−25 °C were used, namely 0, 35, 43, 58, 75, and 98%. The saturated salt solutions were P_2O_5, $CaCl_2{\cdot}6H_2O$, $K_2CO_3{\cdot}2H_2O$, $NaBr{\cdot}2H_2O$, NaCl, and $CuSO_4{\cdot}5H_2O$, respectively. Conditioning was achieved for at least 2 weeks to ensure the equilibration of the water content in the films with that of the atmosphere (stabilization of the sample weight).

Thermogravimetric Analysis. Thermogravimetric analysis was used to accurately determine the water content of the films conditioned at different relative humidities. The measurements were achieved with a Perkin-Elmer TGA7 instrument. A few milligrams of the sample was heated from room temperature up to 130 °C at 5 °C/min under nitrogen flow (flow rate 20 mL/min). The temperature was subsequently stabilized for 1 h. The loss of weight, ascribed to the water content, was measured for different water activities (water activity = % conditioning relative humidity/100) of the samples.

Water Uptake. The kinetics of water absorption was determined for all compositions. The specimens used were thin rectangular strips with dimensions of 10 mm × 10 mm × 1 mm. The films were therefore supposed to be thin enough so that the molecular diffusion was considered to be one-dimensional. Samples were first dried overnight at 100 °C. After weighing, they were conditioned at 20−25 °C in a desiccator containing sodium sulfate to ensure a RH ratio of 98%. The conditioning of samples in high moisture atmosphere was preferred to the classical technique of immersion in water, because starch is very sensitive to liquid water and can partially dissolve after long time exposure to water. The samples were removed at specific intervals and weighed using a four-digit balance. The water content or water uptake (WU) of the samples was calculated as follows:

$$\mathrm{WU}\ (\%) = \frac{M_t - M_0}{M_0} \times 100 \tag{1}$$

where M_t and M_0 are the weights of the sample after t min exposure to 98% RH and before exposure to high moisture content, respectively.

The mean moisture uptake of each sample was calculated for various conditioning times (t). The mass of water sorbed at time t, $(M_t - M_0)$, can be expressed as[37]

$$\frac{M_t - M_0}{M_\infty} = 1 - \sum_{n=0}^{\infty} \frac{8}{(2n+1)^2\pi^2} \exp\left[\frac{-D(2n+1)^2\pi^2 t}{4L^2}\right] \tag{2}$$

where M_∞ is the mass sorbed at equilibrium, $2L$ the thickness of the polymeric film, and D the diffusion coefficient. At short times, eq 2 can be written as

$$\frac{M_t - M_0}{M_\infty} = \frac{2}{L}\left(\frac{D}{\pi}\right)^{1/2} t^{1/2} \tag{3}$$

At $(M_t - M_0/M_\infty) \leq 0.5$, the error in using eq 3 instead of eq 2 to determine the diffusion coefficient is on the order of 0.1%.[38]

Microscopies. Transmission electron microscopy (TEM) observations were achieved with a Philips CM200 electron microscope operating at 80 kV. A drop of a dilute suspension of cellulose whiskers was deposited and allowed to dry on a carbon-coated grid, previously irradiated with a UV lamp.

Scanning electron microscopy (SEM) was performed to investigate the morphology of the nanocomposite films with a JEOL JSM-6100 instrument. The specimens were frozen under liquid nitrogen, then fractured, mounted, coated with gold/palladium on a JEOL JFC-1100E ion sputter coater, and observed. SEM micrographs were obtained using 7 kV secondary electrons.

Differential Scanning Calorimetry (DSC). Differential scanning calorimetry (DSC) was performed with a Perkin-Elmer DSC7 equipment, fitted with a cooler system using liquid nitrogen. It was calibrated with an indium standard. Conditioned samples were placed in pressure-tight DSC cells, and at least three individual measurements were made to ensure reproducibility. Each sample was heated from −100 to +250 °C at a heating rate of 10 °C/min. The melting temperature (T_m) was taken as the peak temperature of the melting endotherm while the glass transition temperature (T_g) was taken as the inflection point of the specific heat increment at the glass−rubber transition.

Contact Angle Measurements. Contact angle measurements were achieved in order to evaluate the selective affinity of the natural polymers used (amylopectin and cellulose) with the plasticizers (water and glycerol). Solid pure amylopectin and tunicin whisker films were obtained by evaporation. Drops of glycerol or water were deposited on the solid polymeric surface. The contact angles were measured with a CCD camera and processed by an image analysis video card which calculated θ (contact angle) automatically using an image analysis setup. This image analyzer determines the diameter, D, and the height, h, of the solvent droplet in order to evaluate the contact angle following eq 4.

$$\tan\left(\frac{\theta}{2}\right) = \frac{2h}{D} \tag{4}$$

Measurements were performed by static mode on the starch surface and by dynamic mode on the cellulose surface.[39,40]

The Owens−Wendt approach[41] was used to estimate the surface energy (polar and dispersive components) of the amylopectin and cellulose surface. It is worth noting that the

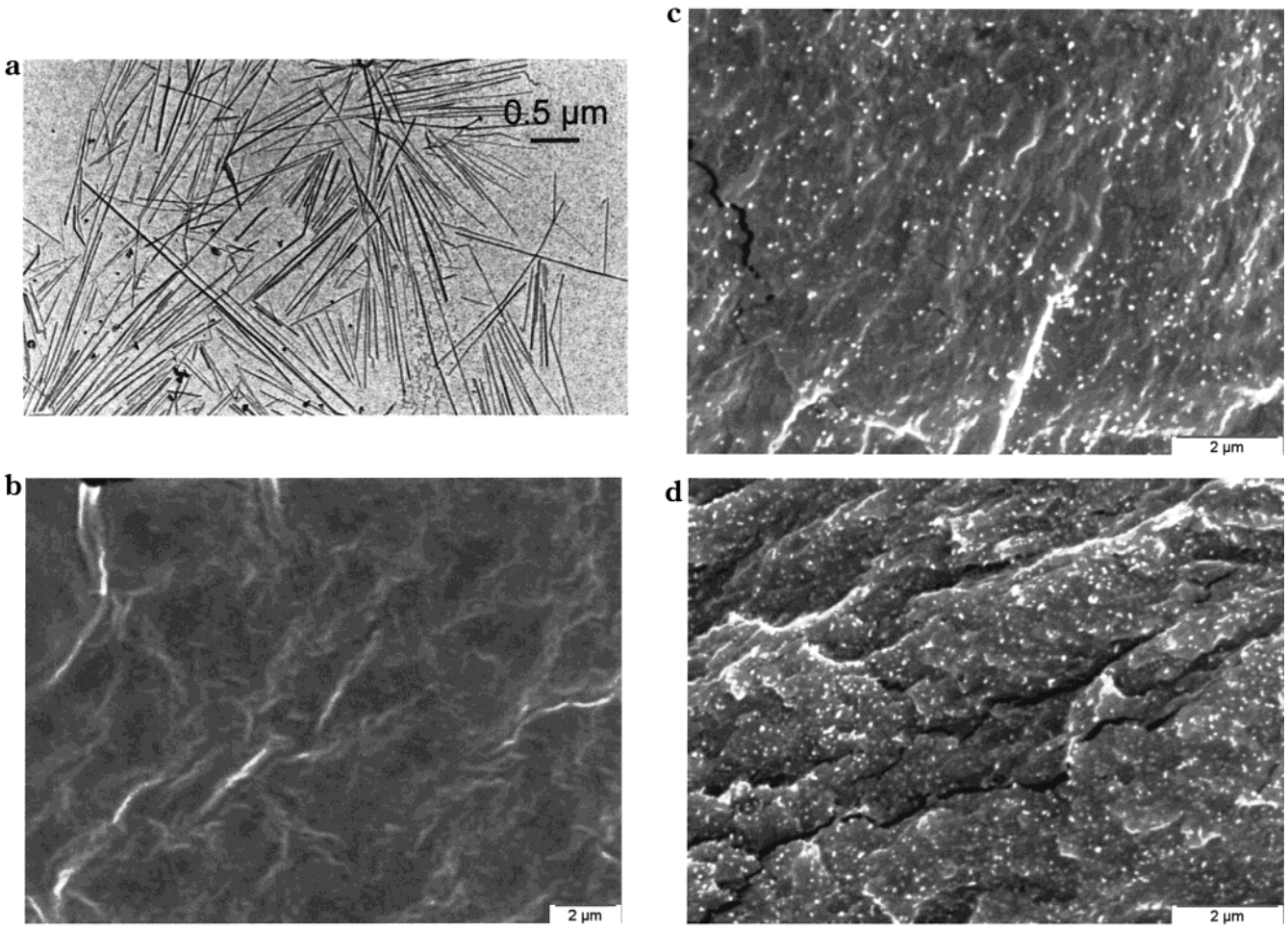

Figure 1. (a) Transmission electron micrograph from a dilute suspension of tunicin whiskers. Scanning electron micrographs from the fractured surfaces of (b) unfilled plasticized starch matrix and related composites filled with (c) 6.2 wt % and (d) 25 wt % tunicin whiskers.

results are only rough estimate of these values because this method generally requires several (up to three) test solutions. For our experiments, only two solutions, water and glycerol, were used.

X-ray Diffraction. Wide-angle X-ray scattering (WAXS) patterns were measured in reflection with a diffractometer using a static detector (SIEMENS D500). Conditioned films were mounted on a poly(methyl methacrylate) (PMMA) hollow support and sealed with a thin aluminum foil in order to preserve moisture conditions during the experiment as explained elsewhere.[31] Samples were exposed for a period of 20 s for each angle of incidence using a Cu $K\alpha_1$ X-ray source with a wavelength of 1.5406 Å operating at 40 kV and 20 mA. The angle of incidence was varied between 8° and 40° by steps of 0.05°. Periodical distances (d) of the main peaks were calculated according to Bragg's law.

Results and Discussion

Morphological Characterization of Tunicin Whiskers. A transmission electron micrograph obtained from a dilute suspension of tunicin whiskers is presented in Figure 1a. The suspension is constituted of individual cellulose fragments consisting of slender parallelepiped rods that have a broad distribution in size. These fragments have a length ranging from 500 nm up to 1−2 μm, and they are almost 10 nm in width. The average aspect ratio (L/d, L being the length and d the diameter) of these whiskers is therefore around 50−200. It was estimated elsewhere[13,14] to be close to 70.

Morphological Characterization of Nanocomposite Films. To evaluate the morphology of the tunicin whiskers/plasticized starch materials, examination of the surface of fractured films was carried out using SEM. Parts b, c, and d of Figure 1 show the fractured surface of unfilled plasticized starch and nanocomposite films filled with 6.2 and 25 wt % cellulose whiskers, respectively. By comparing the micrographs showing the surface of fracture of unfilled starch and of composites, it is easy to identify cellulose whiskers. In fact, tunicin whiskers appear like white dots. Their concentration is a direct function of the cellulose composition in the composite. These shinny dots correspond to the transversal sections of the cellulose whiskers. Their diameters were determined by SEM microscopy and were around 62 ± 2 nm. This value is much higher than the whiskers' diameter. This results from a charge concentration effect due to the emergence of tunicin whiskers from the observed surface. It is worth noting the homogeneous distribution of the filler (cellulose whiskers) within the matrix. The good dispersion level of the filler within the matrix should result in optimal and improved mechanical performance of the composites as commented in the second part of the present article.[19]

Thermogravimetric Analysis. Thermogravimetric analysis (TGA) was used to determine the water content of the various samples. Figure 2 displays the evolution of the desorbed water content versus water activity upon temperature conditions imposed during TGA experiments and described in the Experimental Section for

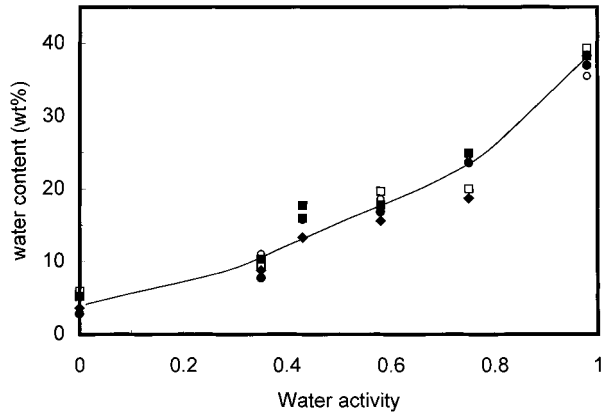

Figure 2. Comparison of water content determined from TGA experiments versus water activity for glycerol plasticized waxy maize starch filled with 0 (●), 3.2 (○), 6.2 (■), 16.7 (□), and 25 wt % (♦) tunicin whiskers.

both unfilled and filled with tunicin whiskers plasticized starch. We ascertain that for all the samples the desorbed water content increases as the water activity of conditioning saturated salt solutions (a_w) increases, but following different behaviors.

Three well-separated zones are displayed in Figure 2. At low water activity ($0 < a_w < 0.35$), the water content increases slightly, and the curves corresponding to the different loading levels are very similar and tend to merge into a single curve. The water content is lower than 10 wt % whatever the composition may be. At intermediate water activity ($0.35 < a_w < 0.75$), the water content increases more rapidly. This is ascribed to the fact that for this water activity range the glass−rubber transition of the plasticized starch matrix probably becomes lower than room temperature at which the samples were conditioned. The concomitant increase in the free volume generates an increased mobility of water molecules within the entangled amylopectin network. In this water activity range again, no obvious difference of behavior is observed as a function of the cellulose whiskers content, and the water content varies from ∼10 to ∼25 wt % as the water activity varies from 0.35 up to 0.75. However, for highly filled samples the water content seems to be lower than for poorly filled ones. This observation is more pronounced for $a_w = 0.75$. This can be ascribed to either an increase of the crystallinity or an increase of the glass−rubber transition temperature of starch material in the presence of cellulose whiskers. In both cases, it should result in a decrease of the mobility of water molecules. At high water activity ($a_w > 0.75$), the desorbed water content continues to increase more rapidly, and the previously difference reported between highly and poorly filled composites tones down.

Water Uptake. In sorption kinetics experiments, the mass of sorbed penetrant is measured as a function of time. The water uptake during exposure to 98% RH of the various cellulose whiskers/plasticized starch composites versus time was evaluated. It was observed that each composition absorbed water during the experiment. The diffusivity of water is strongly influenced by the microstructure of the material, such as the porosity that can develop during drying and also by the water affinity of the polymer components.[42] Moreover, the addition of plasticizers generally increases gas, water, and solute permeability of the film.[43] The change in weight during conditioning at 98% RH is plotted against time in Figure 3. These swelling data are means of several trials, and the reliability of measurements was very good. Two well-separated zones are displayed in Figure 3. At lower times (zone I: $t < 100$ h), the kinetics of absorption is fast, whereas at extended times the kinetics of absorption is slow and leads to a plateau (zone II). In zone I, no clear trend is observed with respect to the cellulose whiskers content. In zone II, the water uptake reaches a plateau, which corresponds to the water uptake at equilibrium.

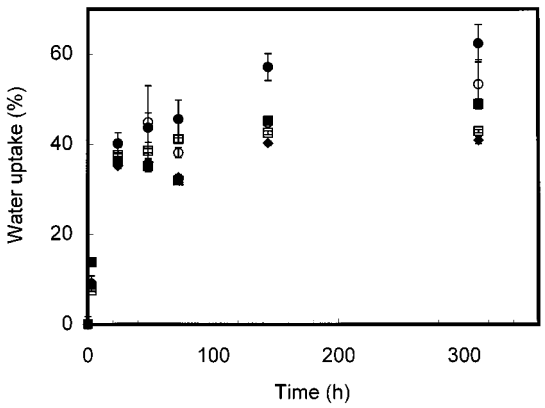

Figure 3. Water uptake during conditioning at 98% RH versus time for glycerol plasticized waxy maize starch filled with 0 (●), 3.2 (○), 6.2 (■), 16.7 (□), and 25 wt % (♦) tunicin whiskers. Results are the average values of triplicates and 95% confidence intervals are reported.

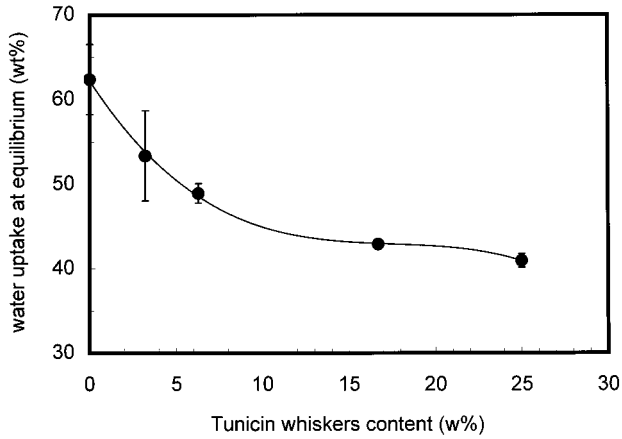

Figure 4. Maximum relative water uptake, or water uptake at equilibrium, during conditioning at 98% RH for glycerol plasticized waxy maize starch filled with tunicin whiskers versus whiskers content. The solid line serves to guide the eye. Results are the average values of triplicates, and 95% confidence intervals are reported.

The water uptake at equilibrium versus cellulose composition is plotted in Figure 4. It is observed that unfilled starch absorbs around 62% water. It corresponds to ∼1.6 g of water per gram of starch. The water uptake at equilibrium decreases as the tunicin whisker content increases. It is only ∼40% for the 25 wt % tunicin whiskers filled composite. Therefore, the swelling of the material is reduced in the presence of cellulose whiskers within the plasticized starch system. Similar results were reported with cellulose microfibril-filled starch.[11,12] This phenomenon was ascribed to the formation of a microfibril network, which prevented the swelling of the starch and therefore its water absorption. However, it is worth noting that the structure of cellulose whiskers completely differs from that of the microfibrils. The former occur as rigid and geometrically

Table 1. Water Diffusion Coefficients in Cellulose Whiskers/Plasticized Starch Composites Conditioned at 98% RH

whiskers content (wt %)	water diffusion coeff ($cm^2/s \times 10^9$)	whiskers content (wt %)	water diffusion coeff ($cm^2/s \times 10^9$)
0	1.76	16.7	1.69
3.2	1.53	25	1.59
6.2	1.47		

well-defined rods, whereas the latter consist of soft and roughly individualized hairy-shaped fillers. The decreased water sensitivity of cellulose filled starch should consequently result, at least partially, from another phenomenon. This could include a decrease of the amylopectin chains mobility, resulting from an increase of the glass−rubber transition temperature or an increase of the crystallinity.

The water diffusivity or diffusion coefficient, D, of water in the starch-based material was estimated using eq 3. The plots of $(M_t - M_0)/M_\infty$ as a function of $(t/L^2)^{1/2}$ were performed for all the compositions and for $(M_t - M_0)/M_\infty \leq 0.5$. The diffusion coefficients were calculated from the slope of these plots. The water diffusion coefficients of the unfilled matrix and reinforced composites are collected in Table 1. The unfilled plasticized starch matrix displays the highest diffusion coefficient. Adding cellulose whiskers within the starch matrix results first in a decrease of D value from 1.76×10^{-9} $cm^2\ s^{-1}$ for unfilled starch up to $1.47 \times 10^{-9}\ cm^2\ s^{-1}$ for the 6.2 wt % filled system. This observation agrees with previous results obtained for cellulose microfibrils/starch composites. This phenomenon was ascribed to the presence of a three-dimensional intertwined cellulose microfibrils network within the matrix, resulting from the establishment of strong hydrogen bonds between cellulose microfibrils which can develop during the evaporation step. This network tends to stabilize the starch matrix when it is submitted to strong moisture conditions. At higher loading level, the previous trend is not clear, and an inverse dependence with the whiskers addition is observed.

Thermal Analysis. Differential scanning calorimetry (DSC) measurements were performed on plasticized starch matrix and related tunicin whiskers filled composites conditioned at various relative moisture contents.

Starch/Glycerol Matrix. Figure 5 shows the DSC traces of glycerol plasticized starch matrix conditioned at 0 and up to 75% RH. All samples display two distinct ill-defined (as least for this heat capacity scale) specific heat increments. Expended views (not shown) of the apparently flat low-temperature DSC traces were performed to precisely analyze these events. The temperatures associated with the midpoints of these two calorimetric transitions are plotted in Figure 6 (filled circles) as a function of the water content.

The low-temperature specific heat increment is located between −47 and −98 °C depending on the moisture content. A relaxation process in glycerol plasticized potato starch was observed by Lourdin et al.[44] in this temperature range using dynamic mechanical analysis. It was assigned to the combination of a secondary relaxation of starch and the main relaxation of the water−glycerol mix. Secondary relaxation processes have been observed by several authors in a range of gelatinized and granular solid starches. They were assigned to either an increase in mobility of water in

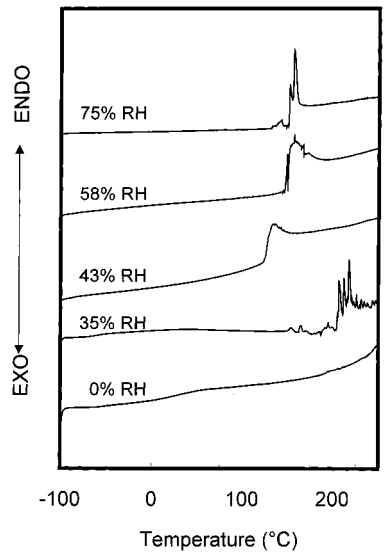

Figure 5. DSC thermograms of glycerol plasticized waxy maize starch for various moisture contents. The relative humidity conditions are indicated in the figure.

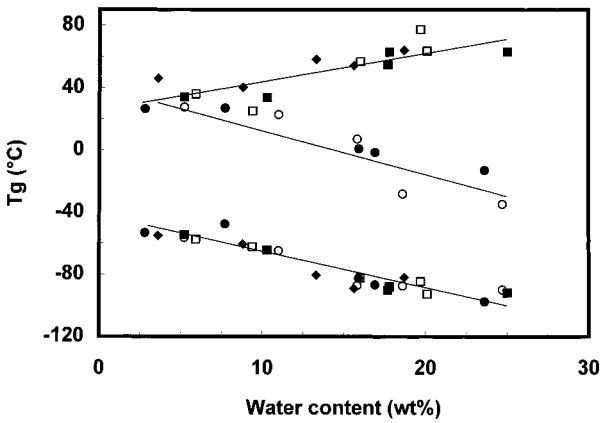

Figure 6. Glass−rubber transition temperatures associated with the midpoints of the transitions versus water content for glycerol plasticized waxy maize starch filled with 0 (●), 3.2 (○), 6.2 (■), 16.7 (□), and 25 wt % (♦) tunicin whiskers. Solid lines serve to guide the eye.

starch[45] or small motions of the chain backbone and rotation of methylol groups.[36] However, it is worth noting that secondary relaxations are not detectable by DSC. It was reported that at high glycerol content (12% and up) this relaxation process was mainly due to glycerol.[45] We suggest assigning this low-temperature transition to the glass−rubber transition of glycerol-rich domains.

The high-temperature specific heat increment is observed from 27 to −13 °C depending on the moisture content. It is ascribed to the glass−rubber transition of amylopectin-rich domains. The waxy maize starch−glycerol matrix appears therefore to be a complex system composed of glycerol-rich and amylopectin-rich domains. The average composition of these two distinct domains can be estimated, at least for water-free material, using the Fox equation. Taking the extrapolated value of Orford et al.[46] for T_g (∼500 K) of starch and the experimental value for T_g of glycerol as determined from DSC measurements (∼194 K), it leads to glycerol-rich domains containing around 20 wt % amylopectin and to amylopectin-rich domains composed of about 65 wt % amylopectin. These values have to be

compared to the mean value, assuming a homogeneous distribution of glycerol within starch, of 67 wt % amylopectin. This obvious aberration clearly shows that the Fox equation is unsuitable for this polymer/solvent system. This inadequacy results from expected strong interactions between both components. Dynamic mechanical measurements performed on this system in the second part of this paper[19] support the idea that this heterogeneous system should be visualized as a blend composed of glycerol-rich domains included in an amylopectin-rich matrix.

Both events strongly depend on the water content, and their temperature decreases as the moisture content increases, displaying a classical plasticizing effect of water. This phenomenon tends to stabilize at high moisture content, because no significant evolution of both transitions is observed between 15 and 25% water content.

For low water content plasticized starch (up to 35% RH), the flat shape of the DSC trace (Figure 5) is an indication of the amorphous state of the material. At increasing moisture content, an endothermal peak appears. Its temperature position first increases with water content, from ~130 °C for samples conditioned at 43% RH up to ~155 °C for samples conditioned at 58% RH. At increasing moisture content, it tends to stabilize. This first-order transition is attributed to the melting of water-induced crystalline amylopectin domains. Indeed, it is well-known that during storage gelatinized starch can convert from a noncrystallized form to a crystalline form. This event, known as retrogradation, results from the reassociation of amorphous starch or starch with a low degree of ordering into a more ordered state. This phenomenon includes the formation of short-range ordering such as the formation of single and double helices, gelation, the formation of entanglements or juncture points, and the crystallization of aggregates of helical structures. This reorganization and crystallization of the amylopectin molecules is favored by the plasticization effect induced by water.[47,48] This increase in crystallinity of starches when submitted to increased moisture conditions was also supported by X-ray diffraction experiments.[31,49,50] At high water contents, the amylopectin is thought to form both inter- and intramolecular double helices. The displacement of the endothermal peak toward higher temperatures when the water content increases is probably due to the formation of larger crystal domains as a result of increased mobility of amorphous chains. In addition, increasing crystallinity of the amylopectin lowers the mobility of the amylopectin, resulting in a reinforcement of the network by the formation of physical cross-links and a stabilization of the retrogradation phenomenon.

Tunicin Whisker/Plasticized Starch Composites. The thermal behavior of tunicin whiskers-based composites was also characterized by DSC measurements. The DSC traces again show two glass−rubber transitions as, already, observed for the starch matrix. The temperature associated with the midpoints of these two calorimetric transitions are plotted in Figure 6 as a function of water content for the different compositions. From the knowledge of the thermal behavior of the unfilled glycerol plasticized starch matrix, the low- and high-temperature events were associated with the glass−rubber transition of glycerol- and amylopectin-rich domains, respectively.

T_g of the glycerol-rich fraction decreases as the moisture content increases, similar to what was observed for the unfilled plasticized matrix. For the amylopectin-rich fraction, two distinct trends were observed depending on the tunicin whiskers content. At low loading level (up to 3.2 wt % tunicin whiskers), the classical plasticization effect of water is reported, and T_g decreases as the water content increases following the behavior of the unfilled matrix. For higher cellulose content (6.2 wt % and up), T_g of amylopectin-rich domains significantly increases as the moisture content increases. The apparent unalteration of the evolution of T_g of the glycerol-rich fraction versus water content in the presence of cellulose whiskers results most probably from the fact that these domains occur as inclusions in the continuous phase constituted of amylopectin-rich domains. Therefore, the tunicin whiskers are most probably in direct contact with amylopectin-rich domains rather than glycerol-rich domains when dispersed in the plasticized starch matrix.

Three phenomena could explain the antiplasticization effect of amylopectin-rich domains in the presence of cellulose whiskers.

(i) The first one is due to the likely strong affinity of amylopectin molecules with the reactive cellulose surface. Both components exhibit a high density of hydroxyl groups. This coupling effect could result in a restricted molecular mobility of amylopectin molecules in contact with the whiskers surface. Owing to the very high specific surface of tunicin whiskers, this hindered mobility could be strong enough to affect the global flexibility of the starch matrix.

(ii) The second explanation could be the selective partitioning of glycerol within the material in the presence of cellulose whiskers. One can imagine that glycerol can present higher affinity for the cellulose surface than for the starch-based matrix. A migration of the main plasticizer from the amylopectin-rich domains toward the filler/matrix interface could result, decreasing the plasticizing efficiency of the glycerol for the starch matrix. This phenomenon should result in an increase of T_g and could be emphasized in moist conditions. The selective partitioning of glycerol in poly(vinyl alcohol) (PVA) and hydroxypropylmethylcellulose (HPMC) blends was reported elsewhere.[51]

(iii) Another explanation could be the most likely different crystallization conditions of the glycerol−water−starch system in the presence of the omnipresent cellulose surface in tunicin whiskers-rich composites. A transcrystallization phenomenon was reported for poly(hydroxyoctanoate) in the presence of tunicin whiskers.[18] If such a transcrystallization occurs in the tunicin whisker/starch composites, one can think that it could result in a restricted mobility of amorphous amylopectin chains in the vicinity of the crystallite-coated filler surface, because crystalline domains of amylopectin act as physical cross-links. This hindered molecular mobility of amorphous chains in the amylopectin-rich domains should be emphasized with the water content as a result of the water-induced crystallization.

Though the three mentioned explanations could be involved simultaneously in the observed increase of T_g of the amylopectin-rich fraction of the plasticized starch matrix, an experimental feature supports the last one. Figure 7 shows the DSC traces of moist tunicin whisker/plasticized starch composites (58% RH conditioned samples) for different loading levels. Similar to the

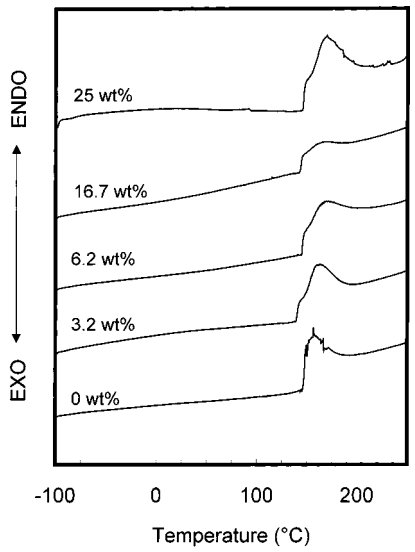

Figure 7. DSC thermograms of 58% RH conditioned tunicin whisker/glycerol plasticized waxy maize starch composites. The tunicin whisker contents are indicated in the figure.

Table 2. Melting Temperatures (°C) of Tunicin Whiskers/ Plasticized Starch Nanocomposite Films Conditioned at Different Moisture Contents

whisker content (wt %)	relative humidity (%)				
	0	35	43	58	75
0			132.6	156.9	156.2
3.2			132.2	158.4	156.2
6.2			131.2	165.1	155.9
16.7			132.0	160.0	156.7
25			134.7	169.5	158.4

unfilled matrix, an endothermic peak attributed to the melting of water-induced crystallites grows as the moisture content increases. This melting endotherm is observed whatever the whiskers content may be. The melting temperatures of these endothermic peaks are collected in Table 2 for all the samples. The heats of fusion were not calculated because of the strong dubiousness for the determination of the baseline.

It is worth noting that the melting endotherm of filled materials exhibits a shoulder on the low-temperature side (Figure 7). This shoulder was also observed for 75% RH conditioned samples. This splitting of the melting endotherm results from the presence of a bimodal distribution of crystallite size. Cellulose most probably acts as a nucleating agent for amylopectin, producing a transcrystalline region around the cellulose whiskers. Orientated crystallization of amylose from a solution on cellulose was previously observed.[52,53] It was shown that the lamellar crystals of amylose grew exclusively on the cellulose to give a "shish kebab" morphology, consisting of a regular system of edge-on amylose crystals organized perpendicular to the cellulose microfibrillar direction. Such a behavior was assigned to a row nucleation phenomenon rather than to a true epitaxial growth. However, the high viscosity of amylopectin-rich domains surrounding the tunicin whiskers limits this phenomenon and restricts the growth of the "shish kebab" structure.

Contact Angle Measurements. The contact angle technique was used in order to quantitatively characterize the affinity of water and glycerol for the amylopectin and cellulose phases. The contact angles measured according to the technique described in the experimental part are collected in Table 3 for the two liquids used (water and glycerol) and the two surfaces (amylopectin and tunicin whisker films). Contact angle values clearly show that both glycerol and water display a higher affinity for the cellulose whisker film surface than for the amylopectin one. The surface energy, as well as the polar and dispersive component values, of the two films was calculated according to the Owens−Wendt approach[41] (Table 4). For both substrates, the polar component is much higher than the dispersive one. This is ascribed to the high density of hydroxyl groups of both polysaccharides. The surface energy is higher for cellulose than for amylopectin.

Table 3. Contact Angle (deg) Values for Water and Glycerol on Amylopectin and Cellulose Whiskers Surface Films

substrate films	water	glycerol
amylopectin	64	72
cellulose whiskers	24	55

Table 4. Total Surface Energy (γ_S), Polar (γ^p), and Dispersive (γ^d) Components of Amylopectin and Cellulose Whisker Films Calculated from the Owens−Wendt Approach

	γ_S (mJ/m^2)	γ^p (mJ/m^2)	γ^d (mJ/m^2)
amylopectin	44.0	42.2	1.8
cellulose whiskers	94.9	94.9	4.9×10^{-6}

These observations tend to show that the localization of the two plasticizers (glycerol and water) is most obviously not homogeneous in the tunicin whiskers/ starch composites. They probably redistribute within the matrix, diffusing toward the cellulose surface. This relocalization decreases the plasticizing effect of glycerol and water in the bulk amylopectin matrix. The main consequence of this redistribution should be the shift of the glass−rubber transition of the amylopectin-rich phase toward higher temperatures in the composites. The accumulation of plasticizer in the cellulose/amylopectin interfacial zones could, in turn, improve the ability of amylopectin chains to crystallize, leading to the formation of a transcrystalline zone around the whiskers.

Wide-Angle X-ray Scattering (WAXS). The nanocomposite films resulting from the casting and evaporation of gelatinized starch were characterized by WAXS. X-ray diffractograms were collected for the different water contents and loading levels in order to determine the evolution of the crystallinity.

Starch/Glycerol Matrix. Wide-angle X-ray diffraction patterns of the unfilled plasticized starch matrix conditioned at 35 and up to 75% RH are presented in Figure 8. The diffractogram recorded for a film of pure cellulose obtained from the evaporation of a tunicin whiskers suspension is added in Figure 8. At low moisture content, the starch film shows no diffraction peak and displays typical behavior of a fully amorphous polymer. It is characterized by a broad hump located around $2\theta = 18°$. This result agrees with DSC measurements.

As the water content increases, the amorphous broad hump shades off progressively, and three ill-defined diffraction peaks, which grow with moisture content, are observed. Their angular locations around $2\theta = 17.2°$, 22.1°, and 23.9° are typical of B-starch structure.[54] The crystalline regions consist therefore of double helices with a loose packing density in the unit cell, water being an integral part of this polymorph. The d values associated with these peaks are 5.20, 4.01, and 3.72 Å, respectively. The semicrystalline nature of moist plas-

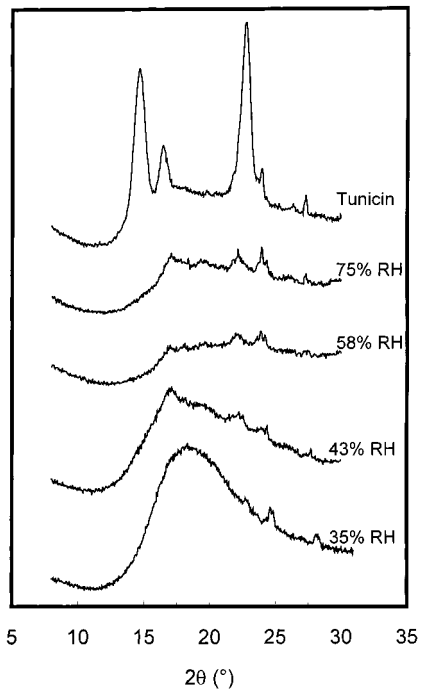

Figure 8. Wide-angle X-ray diffraction patterns of glycerol plasticized waxy maize starch for various moisture contents and tunicin whiskers film. The relative humidity conditions are indicated in the figure.

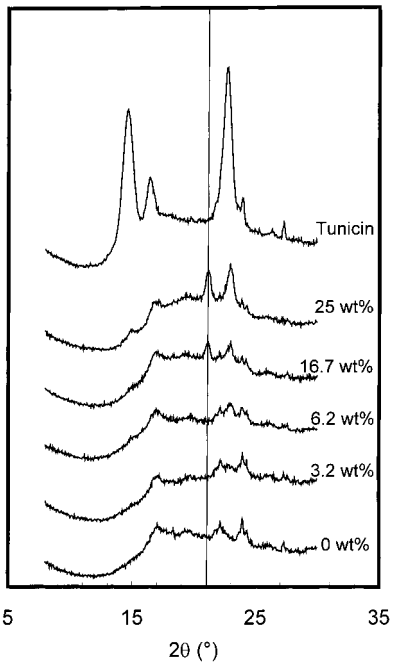

Figure 9. Wide-angle X-ray diffraction patterns of 75% RH conditioned tunicin whisker/glycerol plasticized waxy maize starch composites. The tunicin whisker contents are indicated in the figure.

ticized waxy maize starch films evidenced by WAXS experiments agrees with DSC results. The tunicin whiskers film displays three well-defined peaks around $2\theta = 14.6°$, 16.4°, and 22.7°. The d values associated with these peaks are 6.06, 5.40, and 3.91 Å, respectively. They are typical of cellulose I. The relative magnitude of these peaks depends on the whiskers orientation in the film.

Tunicin Whisker/Plasticized Starch Composites. Diffractograms of the highly moist (75% RH) nanocomposite materials are shown in Figure 9. Diffraction patterns of unfilled plasticized starch and tunicin whiskers films are added as references. The diffractograms of the various cellulose/starch composites consist in a superimposition of the diffractograms of the two parent components balanced by the composition.

However, it is worth noting that for the films filled with 16.7 and 25 wt % of cellulose whiskers, a new well-defined diffraction peak located around $2\theta = 21.15°$ (corresponding to the vertical line) is observed, whose intensity increases with cellulose content. The d value associated with this peak is 4.2 Å. This diffraction peak arises neither from the unfilled plasticized starch nor from the tunicin. Because tunicin whiskers are well-defined objects, which crystallinity should not be changed when dispersed in the matrix, this new peak arises most probably from amylopectin. This specific crystallinity occurs, or at least is detectable, in amylopectin only in highly moist conditions and in the presence of a high tunicin whiskers content.

To yield the specific character of this peak, a modeling of the X-ray diffractograms was performed from the combination of the diffractograms of the pure parent components. A simple mixing rule was used to build up the theoretical diffractograms. Both experimental and theoretical wide-angle X-ray diffraction patterns are shown in parts a, b, c, and d of Figure 10 for highly filled nanocomposites (25 wt % tunicin whiskers), conditioned at 35, 43, 58, and 75% RH, respectively. The theoretical curve fits very well the experimental data at 35% RH (Figure 10a). At higher moisture content (43 and 58% RH, Figure 10, b and c), the fit is satisfactory, except for the cellulose peak located around $2\theta = 14.6°$, for which the predicted magnitude is much higher than the experimental one. This probably results from the different orientation of tunicin whiskers within the film obtained from only cellulose and from the composite. The whiskers distribution is most likely random in the composite contrarily to the reference whisker films, which is composed of in-plane oriented filler. The same trend is reported between the experimental and predicted X-ray diffraction patterns of composites conditioned at 75% RH (Figure 10d), but the most significant difference between these two diffractograms is the total absence of the peak at $2\theta = 21.15°$ ($d = 4.2$ Å) in the predicted diffractogram. Similar differences between experimental and predicted X-ray diffraction patterns were obtained for the glycerol plasticized starch filled with 16.7 wt % tunicin whiskers.

This observation could probably be interpreted as an interfacial effect in relation with the shoulder observed on the low-temperature side of the melting endotherm by DSC for similar conditions. This again could be interpreted as a transcrystallization phenomenon of amylopectin on the surface of the cellulose whiskers. The whiskers could act as nucleation points, and owing to the steric obstacles due to the high whiskers content, distortion of amylopectin crystallites occurs. However, the experimental evidence of the transcrystallinity cannot be displayed by classical techniques, such as optical microscopy because of the dimensions of the tunicin whiskers.

Regarding the nature of the crystallized structure giving the diffraction peak at $2\theta = 21.15°$, it is doubtful. However, it is well-known that amylopectin crystallizes readily and forms complexes with glycerol detectable by X-ray diffraction or other methods. The peak at $2\theta =$

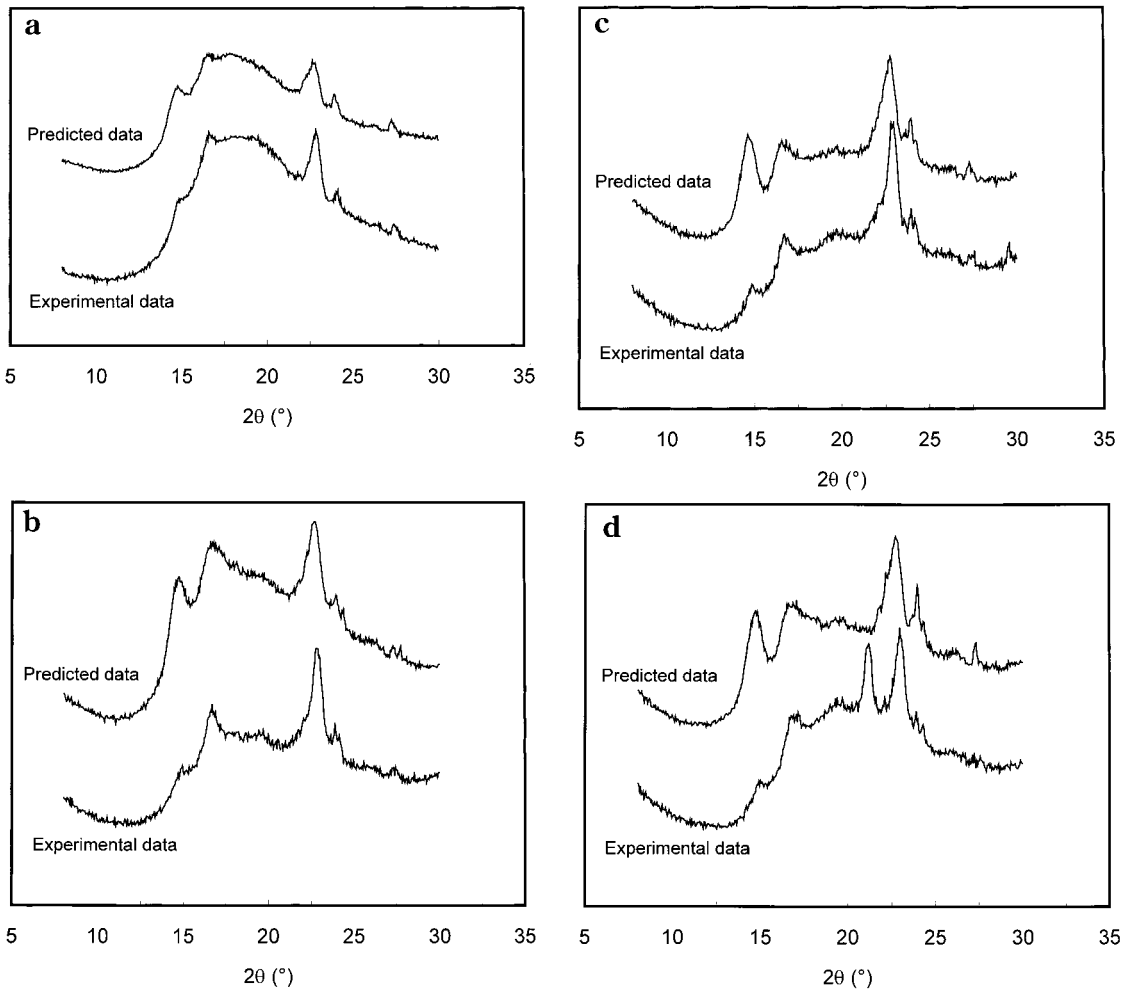

Figure 10. Experimental and predicted wide-angle X-ray diffraction patterns of 25 wt % filled tunicin whiskers/glycerol plasticized waxy maize starch composites conditioned at (a) 35, (b) 43, (c) 58, and (d) 75% RH.

21.15° could probably be assigned to a glycerol−starch V structure, but it does not correspond to not any reported structure. Since the V form is a single helix, it appears that the 4.2 Å is not from the double-helix B form. Further experiments are necessary to confirm this hypothesis.

Conclusions

Nanocomposite materials were obtained from glycerol plasticized waxy maize starch as the matrix and a suspension of tunicin—an animal cellulose—whiskers as a model reinforcing phase. The unfilled matrix appears as a complex heterogeneous system composed of glycerol-rich domains dispersed in an amylopectin-rich continuous phase. Each phase exhibits its own glass−rubber transition, for which the temperature decreases as the moisture content increases owing to the plasticizing effect of water. This lowering of T_g induces the crystallization of the matrix at room temperature (retrogradation phenomenon) when the water content increases.

Significant changes occur in the composite systems when tunicin whiskers are homogeneously dispersed in this complex matrix. All results lead to the conclusion that both plasticizers (glycerol and water) redistribute within the matrix, diffusing toward the cellulose surface. This relocalization effect decreases the plasticizing effect of glycerol and water in the bulk amylopectin matrix, resulting in an increase of the T_g of amylopectin-rich domains. The accumulation of plasticizer in the cellulose/amylopectin interfacial zones improves the ability of amylopectin chains to crystallize, leading to the formation of a possible transcrystalline zone around the whiskers. These specific crystallization conditions have been evidenced at high moisture content and high whiskers content (>16.7 wt %) by DSC and WAXS. It is displayed through a shoulder on the low-temperature side of the melting endotherm and the observation of a new peak in the X-ray diffraction pattern. This transcrystalline zone could originate from a glycerol−starch V structure. This inherent restricted mobility of amylopectin chains most likely accounts for the lower water uptake of cellulose/starch composites for increasing filler content.

Acknowledgment. The authors gratefully acknowledge Roquette S.A. for supplying waxy maize starch, Dr. H. Chanzy for stimulating discussions, Dr. M. Paillet and Y. Minot for their help in film processing, Mr. L. Fouchet for his help in contact angle, Mrs. D. Dupeyre and Mr. R. Vuong for their help in SEM and TEM microscopy, respectively, and Zebda for moral support. The authors are indebted to ADEME (Agence Française de l'Environnement et de la Maîtrise de l'Energie) for financial support (ADEME/CNRS convention # 99 01 033).

References and Notes

(1) Griffin, G. J. L. US Patent 4,016,177, 1977.
(2) Griffin, G. J. L. US Patent 4,021,388, 1977.

(3) Griffin, G. J. L. US Patent 4,125,495, 1978.
(4) Westhoff, R. P.; Otey, F. P.; Mehltretter, C. L.; Russell, C. R. *Ind. Eng. Chem. Prod. Res. Dev.* **1974**, *13*, 123.
(5) Otey, F. P.; Westhoff, R. P.; Russell, C. R. *Ind. Eng. Chem. Prod. Res. Dev.* **1977**, *16*, 305.
(6) Otey, F. P.; Westhoff, R. P. US Patent 4,133,784, 1979.
(7) Otey, F. P.; Westhoff, R. P. US Patent 4,337,181, 1982.
(8) Otey, F. P.; Westhoff, R. P.; Doane, W. M. *Ind. Eng. Chem. Prod. Res. Dev.* **1987**, *26*, 1659.
(9) Wiedmann, W.; Strobel, E. *Starch* **1991**, *43*, 138.
(10) Stepto, R. F.; Dobler, B.; Silbiger, J. European Patent 0,326,-517, 1989.
(11) Dufresne, A.; Vignon, M. R. *Macromolecules* **1998**, *31*, 2693.
(12) Dufresne, A.; Dupeyre, D.; Vignon, M. R. *J. Appl. Polym. Sci.* **2000**, *76*, 2080.
(13) Favier, V.; Canova, G. R.; Cavaillé, J. Y.; Chanzy, H.; Dufresne, A.; Gauthier, C. *Polym. Adv. Technol.* **1995**, *6*, 351.
(14) Favier, V.; Cavaillé, J. Y.; Chanzy, H. *Macromolecules* **1995**, *28*, 6365.
(15) Helbert, W.; Cavaillé, J. Y.; Dufresne, A. *Polym. Compos.* **1996**, *17*, 604.
(16) Dufresne, A.; Cavaillé, J. Y.; Helbert, W. *Polym. Compos.* **1997**, *18*, 198.
(17) Dubief, D.; Samain, E.; Dufresne, A. *Macromolecules* **1999**, *32*, 5765.
(18) Dufresne, A.; Kellerhals, M. B.; Witholt, B. *Macromolecules* **1999**, *32*, 7396.
(19) Anglès, M. N.; Dufresne, A. Submitted to *Macromolecules*.
(20) Davies, H. A.; Wolff, I. A.; Cluskey, J. E. US Patent 2,656,-571, 1953.
(21) Muetgeert, J.; Hiemstra, P. US Patent 2,822,581, 1958.
(22) Walton, H. M. US Patent 3,312,560, 1967.
(23) Protzman, T. F.; Wagoner, J. A.; Young, A. H. US Patent 3,-344,216, 1967.
(24) Sommerfeld, H.; Blume, R. *J. Chem. Educ.* **1992**, *69* (5), A151.
(25) Svegmark, K.; Hermansson, A. M. *Food Struct.* **1993**, *12*, 181.
(26) Van Soest, J. J. G.; De Wit, D.; Tournois, H.; Vliegenthart, J. F. G. *Polymer* **1994**, *35*, 4722.
(27) Hulleman, S. H. D.; Janssen, F. H. P.; Feil, H. *Polymer* **1998**, *39*, 2043.
(28) Pellegrini, C.; Tomka, I. *Macromol. Symp.* **1998**, *127*, 31.
(29) Wise, L. E.; Murphy, M.; D'Addiecco, A. A. *Pap. Trade J.* **1946**, *122*, 35.
(30) Marchessault, R. H.; Morehead, F. F.; Walter, N. M. *Nature* **1959**, *184*, 632.
(31) Buléon, A.; Bizot, H.; Delage, M. M.; Pontoire, B. *Carbohydr. Polym.* **1987**, *7*, 461.
(32) Trommsdorff, U.; Tomka, I. *Macromolecules* **1995**, *28*, 6128.
(33) Trommsdorff, U.; Tomka, I. *Macromolecules* **1995**, *28*, 6138.
(34) Lourdin, D.; Coignard, L.; Bizot, H.; Colonna, P. *Polymer* **1997**, *38*, 5401.
(35) Bizot, H.; Le Bail, P.; Leroux, B.; Davy, J.; Roger, P.; Buléon, A. *Carbohydr. Polym.* **1997**, *32*, 33.
(36) Butler, M. F.; Cameron, R. E. *Polymer* **2000**, *41*, 2249.
(37) Comyn, J. In *Polymer Permeability*; Comyn, J., Ed.; Elsevier Applied Science: New York, 1985.
(38) Vergnaud, J. M. In *Liquid Transport Process in Polymeric Materials: Modeling and Industrial Applications*; Prentice-Hall: Englewood Cliffs, NJ, 1991.
(39) Jallu, J.; Aurenty, P.; Gandini, A. *TAGA Proc., Colorado* **1995**, 1170.
(40) Lanet, V.; Gandini, A. *TAGA Proc., Colorado* **1995**, 1182.
(41) Owens, D. K.; Wendt, R. C. *J. Appl. Polym. Sci.* **1969**, *13*, 1741.
(42) Marousis, S. N.; Karathanos, V. T.; Saravacos, G. D. *J. Food Process. Preserv.* **1991**, *15*, 183.
(43) Gontard, N.; Guilbert, S.; Cuq, J.-L. *J. Food Sci.* **1993**, *58* (1), 206.
(44) Lourdin, D.; Bizot, H.; Colonna, P. *J. Appl. Polym. Sci.* **1997**, *63*, 1047.
(45) Shogren, R. L. *Carbohydr. Polym.* **1992**, *19*, 83.
(46) Orford, P. D.; Parker, R.; Ring, S. G.; Smith, A. C. *Int. J. Biol. Macromol.* **1989**, *11*, 91.
(47) Van Soest, J. J. G.; de Wit, D.; Vliegenthart, J. F. G. *J. Appl. Polym. Sci.* **1996**, *61*, 1927.
(48) De Meuter, P.; Amelrijckx, J.; Rahier, H.; Van Mele, B. *J. Polym. Sci., Polym. Phys.* **1999**, *37*, 2881.
(49) Ramkumar, D. H. S.; Bhattacharya, M. *J. Mater. Sci.* **1997**, *32*, 2565.
(50) Rindlav-Westling, A.; Stading, M.; Hermanson, A. M.; Gatenholm, P. *Carbohydr. Polym.* **1998**, *36*, 217.
(51) Sakellariou, P.; Hassan. A.; Rowe, R. C. *Colloid Polym. Sci.* **1994**, *272*, 48.
(52) Helbert, W.; Chanzy, H. *Carbohydr. Polym.* **1994**, *24*, 119.
(53) Hulleman, S. H. D.; Helbert, W.; Chanzy, H. *Int. J. Biol. Macromol.* **1996**, *18*, 115.
(54) Van Soest, J. J. G.; Hulleman, S. H. D.; de Wit, D.; Vliegenthart, J. F. G. *Ind. Crops Prod.* **1996**, *5*, 11.

MA0008701